Comparative Study of Defected Waveguide Structure with Circuit Modelling

S. J. Chin and M. Z. A. Abd. Aziz
Centre for Telecommunication Research and Innovation,
Faculty of Electronic and Computer Engineering, Universiti Teknikal Malaysia Melaka,
76100 Durian Tunggal, Melaka, Malaysia.
mohamadzoinol@utem.edu.my

***Abstract*— The comparisons of Defected Waveguide Structure (DWS) are made to determine their performances toward waveguide in Ultrawideband (UWB) frequency range. Initially, the copper waveguide is designed to have a basic square structure as DWS. The straight connecting strip is added on in between the square. The straight connecting strip is then folded to reduce the length. All the designs and simulation process are constructed in CST Microwave software. The results of transmission coefficient (S21) and reflection coefficient (S11) are used for performance analysis. An equivalent circuit is designed and simulated in Advanced Design System (ADS) for modelling purpose based on filter concept. Copper waveguide performs as high pass respond with the frequency more than cut off frequency. Basic square DWS operates from 3.5GHz to 8.25GHz. Meanwhile, basic square DWS with straight and meander line connecting strip operate at a higher frequency from 8.11GHz-9.23GHz and 7.68GHz-10.8GHz, respectively. Basic square DWS with meander line connecting strip operates for the wider bandwidth of 3.12GHz with compact size.**

***Index Terms*— Defected Waveguide Structure; Filter Concept; Reflection Coefficient; Transmission Coefficient; Ultrawideband.**

I. INTRODUCTION

The Transmission of the signal can be conducted in wireless or non-wireless form. For the transmission in non-wireless form, the waveguide is one of the potential candidates as it provides low loss and high-power handling. However, it is bulky in size. Today, it has been applied in filter and antenna field [1-2]. Besides that, it is also noticed that metamaterial is designed with waveguide [3-4]. From previous studies, theoretical models are used to study the characteristics of waveguide itself [5-6]. The examples of metamaterial are Electromagnetic Bandgap (EBG) [7-8], Frequency Selective Surface (FSS) [9], Defected Ground Structure (DGS) [10] and Defected Microstrip Structure (DMS) [11]. Defected structure refers to a shape that is designed as a slot or patch at specific location or plane. DGS at ground plane normally consists of one unique design structure such as a modified-T shaped slot in [10]. DMS at microstrip feed line in [11] is designed in reversed T-shape for wideband applications. Yet, there is no information about Defected Waveguide Structure (DWS).

The basic geometry of square is used to design in the waveguide as it is easy to design. The straight connecting strip is then added on between squares. The length of the connecting strip is depended on the gap separation between square. Larger gap separation will increase the length of the waveguide. To reduce the length of the waveguide, meander line technique can be applied at the straight connecting strip. It folds the straight line to become meander structure. The meander line technique has been applied in antenna as it reduces the size and cost [12-13].

This paper studies the effects DWS towards waveguide performance. The basic square DWS, the basic square with the straight connecting strip and the basic square with meander line connecting strip are compared with fully copper waveguide. The results of transmission coefficient (S21) and reflection coefficient (S11) are used to determine their performances. The equivalent circuit is also used as modelling purpose to determine the inductor (L) and capacitor (C) for each design.

II. DEFECTED WAVEGUIDE STRUCTURE DESIGN

The A simple rectangular waveguide is designed to have four walls (sides wall which is left and right, top and bottom walls) by using CST Microwave software. The copper layer is designed at all four inner walls of the waveguide. The width (a) and height (b) of the waveguide can be used to determine the cut off frequency (f_c). Typically, the width of the waveguide is two times of height [14]. The Equation 1 below shows the relationship between waveguide dimension and f_c.

$$f_c = \frac{1}{2\pi\sqrt{\mu\varepsilon}}\sqrt{\left(\frac{m\pi}{a}\right)^2 + \left(\frac{n\pi}{b}\right)^2} \quad (1)$$

As the waveguide dimension, a and b are larger; the longer wavelength can propagate through the waveguide. The material used to construct the rectangular waveguide is FR4. For substrate, the dielectric constant = 4.4, tangent loss = 0.019 and thickness = 1.6mm. The thickness of copper is 0.035mm. The operating frequency for this rectangular waveguide is 3GHz-10GHz for UWB applications. This rectangular waveguide has two open-ended surfaces to design with waveguide port 1 and 2. The rectangular waveguide (Design A) has a dimension of a = 49mm and b = 52mm.

The basic geometry of square is then located at the inner walls of the waveguide. The dimension of the square $W_{sq} \times W_{sq}$ is 6mm x 6mm with total 150 elements of square is used. The number of squares that is designed in waveguide is limited to the width and height of waveguide. Three rows and two rows of squares are designed at both sides, top and bottom walls respectively. Each row has 15 elements of square. At the same time, the length of waveguide is determined by the number of squares and gap separation (G).

Thus, the rectangular waveguide is designed to have basic squares with G = 7mm in between (Design B). The total length of Design B is 198mm.

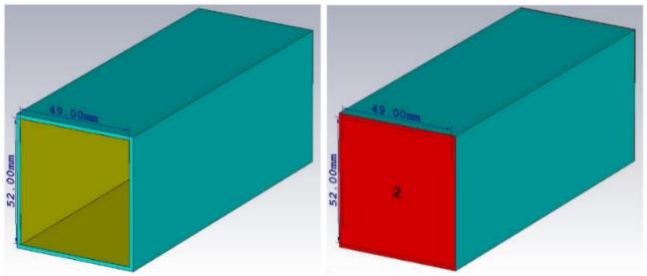

(a) (b)

Figure 1: The perspective view of (a) Design A and (b) waveguide port at both ends of the waveguide

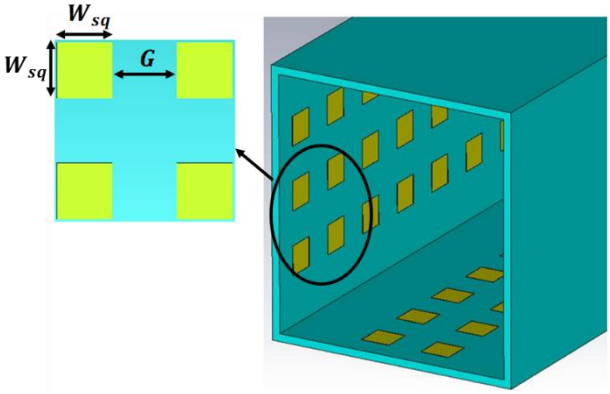

Figure 2: The perspective view of Design B with parameters

The basic squares are then designed with a straight line in between them. The length of connecting strip is directly proportional to the G between squares. The length (L_1) and width (W_1) of connecting strip used are 7mm and 0.3mm respectively. G between the squares can be reduced by folding the straight connecting strip into horizontal and vertical segments. A meander structure which consists of a width W_{ML}= 0.4mm, length L_{ML}= 2.3mm and small gap between square and meander section G_{ML}= 1mm can be observed at the middle of squares in Figure 3. The meander structure is designed to achieve G_1 = 3mm while maintain the original L_1 and W_1 of the straight connecting strip. Meanwhile, the design of basic square DWS with the straight connecting strip (Design C) and basic square DWS with meander line connecting strip (Design D) is showed in Figure 4. The equivalent circuits are then designed and optimized to match with simulated S11 and S21 results for each design. The equivalent circuit are designed based on filter concept in term of L and C [14].

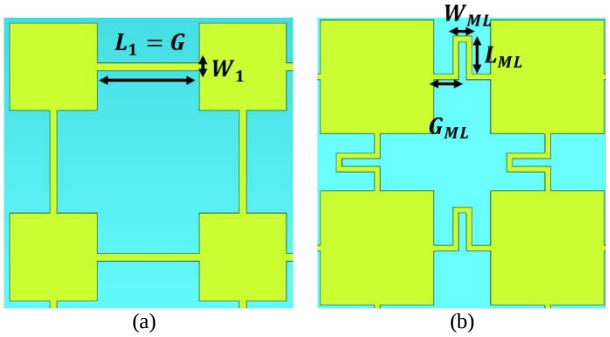

(a) (b)

Figure 3: The view of (a) straight connecting strip and (b) meander line connecting strip

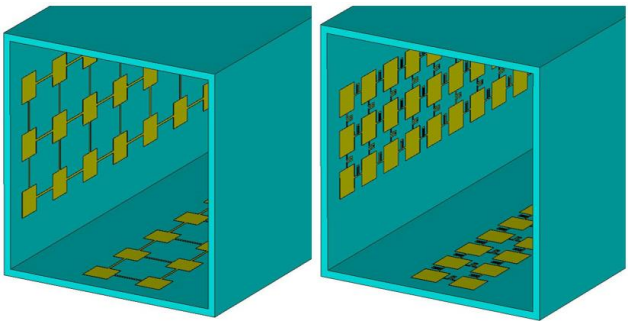

(a) (b)

Figure 4: The perspective view of (a) Design C and (b) Design D

III. RESULT

The designs are simulated in UWB frequency range. The simulation is done by dividing the UWB frequency range into half from 2GHz-6GHz and 6GHz-11GHz. For lower frequency range, the results of 2GHz-5GHz are showed for the significant changes. The fully copper waveguide (Design A) shows high transmission and very low reflection. This proves that fully copper waveguide promises the low loss of signal. At the frequency of 2.76GHz, the S21 = 10dB where it means that frequency bigger than 2.76GHz can be propagated through the waveguide. In lower frequency range, the S21 result performs low pass respond where L1 = 475.4pH is used. The simulated S21 and S11 appear almost in straight line for the higher frequency range. The S21 is equal to zero while S11 shows less than -100dB in Figure 5 (a) (ii). Thus, the equivalent circuit can be represented by a small resistance during the transmission in the waveguide.

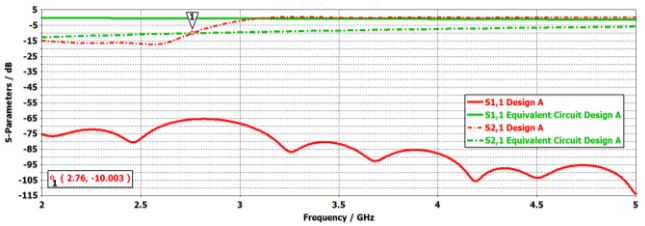

(a) (i)

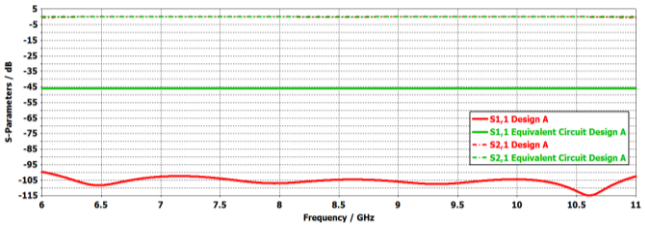

(a) (ii)

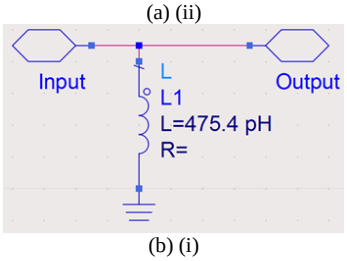

(b) (i)

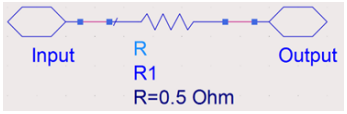

(b) (ii)

Figure 5: The (a) simulated S-parameters and (b) equivalent circuit for Design A at (i) lower and (ii) higher frequency range

Each design will be compared with Design A for reference design in term of S11 and S21. The simulated S11 of Design A is not included for comparison as the value is too small for scaling purpose. Design B shows low pass respond at low-frequency range which is same as Design A. It has lower value of L compare to Design A where L1 = 1.31nH. In the simulation, the S11 and S21 is intercepted at 3GHz. At frequency that is bigger than 3GHz, Design B can operate with highest S21 of -6.37dB at 5GHz.

For higher frequency range, Design B performs passband from 6GHz-8.25GHz. It achieves lowest S21 of -43.86dB at 8.84GHz. Two band stop responds is modelled to achieve the optimized LC value to match with simulation results. The first series of LC tank consists of L1 = 482.2pH and C1 = 644.6fF. Another series LC tank has L2 = 984.5pH and C2 = 323.75fF. Design B creates band stop after frequency 8.25GHz compares to Design A with all pass in the higher frequency range.

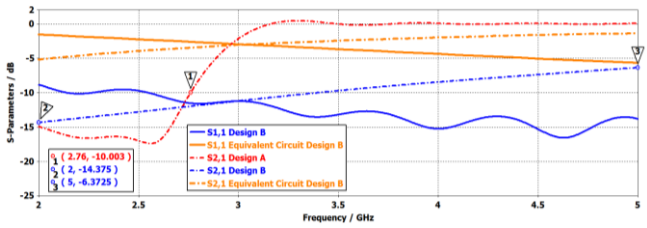

(a) (i)

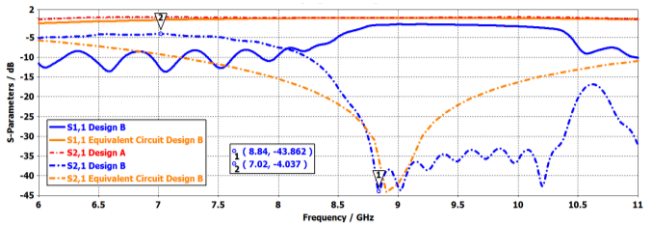

(a) (ii)

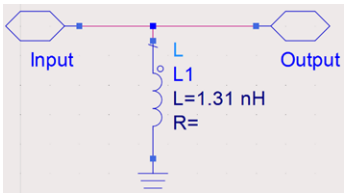

(b) (i)

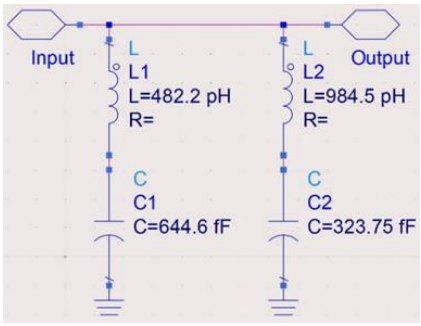

(b) (ii)

Figure 6: The (a) simulated S-parameters and (b) equivalent circuit for Design B at (i) lower and (ii) higher frequency range

For Design C, both lower and higher frequency range contribute one bandpass respond, and one band stop responds with different values. Design C able to work as bandpass in a narrow bandwidth of 2.2GHz-2.28GHz which is different from Design A and B. It performs bandstop in wideband from 2.29GHz-5GHz with lowest S21 of -32.66dB at 2.96GHz. The parallel LC tank provides pass band performance while the series LC tank provides stopband performance. The parallel LC tank consists of L1 = 66.56pH and C1 = 12.77pF. L2 = 112.14pH and C2 = 26.01pF is the value for series LC tank.

The lowest S21 of -36.75dB occurs at 6GHz while highest S21 of -7.03dB occurs at 8.86GHz for the higher frequency range. Design C shows passband from 8GHz-9.25GHz which is different from both Design A and B. Design C starts to operate when Design B stops at a frequency around 8GHz. For the parallel LC tank, L1 = 33.45pH and C1 = 10.4pF. The series LC tank has L2 = 807.4pH and C2 = 0.86pF.

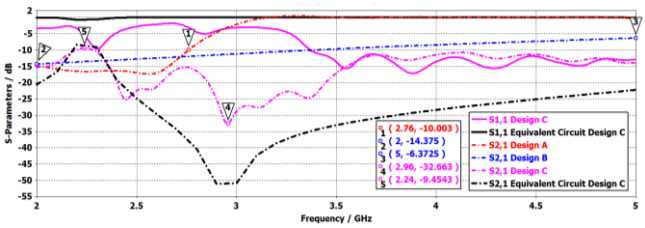

(a) (i)

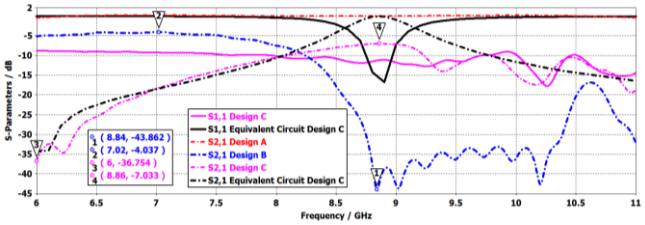

(a) (ii)

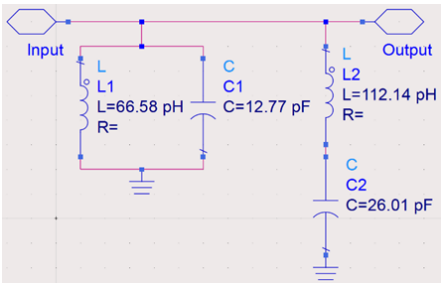

(b) (i)

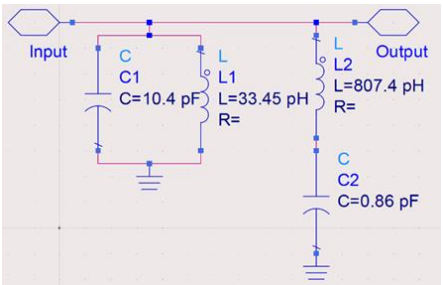

(b) (ii)

Figure 7: The (a) simulated S-parameters and (b) equivalent circuit for Design C at (i) lower and (ii) higher frequency range

It is observed that Design C and D have the same equivalent circuit pattern with almost similar values of L and C. The most obvious is that Design D has shifted the lowest S21 from 2.96GHz of Design C to 3.69GHz. The series LC tank which shows band stop respond contributes to this significant change. The value L2 is decreased to almost half compares to Design C which is 55.22pH whereas the value of C2 is increased slightly to 32.8pF. Design D has also increased the value of L1 and C1 for the bandpass respond to drop the S21 values slightly at the passband bandwidth. The

values of L1 and C1 are increased to 74.26pH and 15.88pF.

The Figure 8 (a) (ii) shows that Design D achieves wider bandwidth from 7.68GHz-10.8GHz compare to Design C which operates from 8.11GHz-9.23GHz. The highest S21 of Design D for higher frequency range is -5.05 dB which occurs at 9.32GHz. The bandpass respond of Design D has slightly drop in values for both L and C compare to Design C. C1 = 10.14pF and L1 = 33.45pH from Design C is decreased to C1 = 9.44pF and L1 = 32.95pH. The lowest S21 is contributed by the band stop respond. As both the Design C and D perform mostly similar characteristics for lowest S21, the band stop respond is achieved with almost similar value. Only the value of L2 is changed slightly to 804.9pH while the value of C2 of 0.86pF remains unchanged.

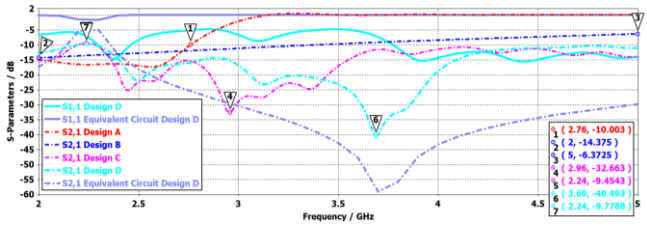

(a) (i)

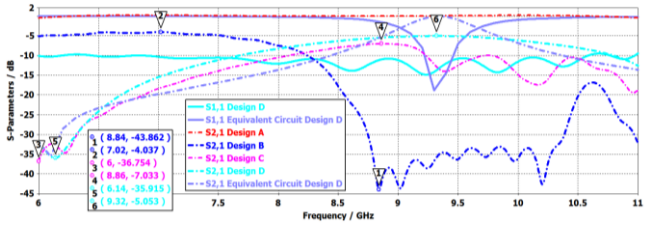

(a) (ii)

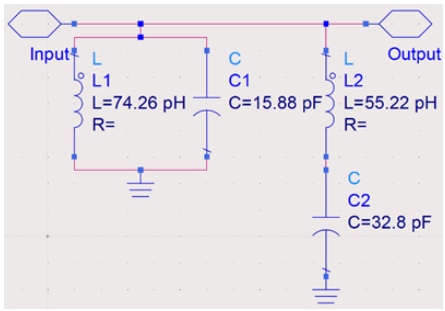

(b) (i)

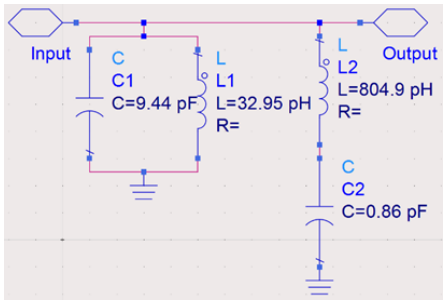

(b) (ii)

Figure 8: The (a) simulated S-parameters and (b) equivalent circuit for Design D at (i) lower and (ii) higher frequency range

Design A which is the fully copper waveguide can operate with the frequency bigger than the cut off frequency. This is because width and height of waveguide determine the cut off frequency. Design B shows bandpass respond from 3.5GHz to 8.25GHz. Meanwhile, Design C and D achieve almost similar operating characteristics. Design C operates from 8.11GHz-9.23GHz while Design D operates from 7.68GHz-10.8GHz. Design D achieves a wider bandwidth of 3.12GHz compares to Design C with 1.12GHz of bandwidth. Design D also shows compact design due to meander line technique used. It shortens the gap separation from initially 7mm to 3mm.

IV. Conclusion

The comparative study of Defected Waveguide Structure, DWS is done in UWB frequency range. Their performances towards waveguide are compared and analyzed in terms of S21 and S11. It is observed that copper waveguide operates with frequency more than cut off frequency. The basic square DWS operates from 3.5GHz-8.25GHz. The basic square DWS with straight and meander line of connecting strip have almost similar performances where they operate at a higher frequency from 8.11GHz-9.23GHz and 7.68GHz-10.8GHz. Basic square DWS with meander line connecting strip operates for the wider bandwidth of 3.12GHz in a compact size. In future, monopole antenna will be located inside all these waveguides with different types DWS to determine the antenna performances.

Acknowledgment

An acknowledgment is given to Universiti Teknikal Malaysia Melaka (UTeM) and Ministry of Higher Education (MOHE) for the support of this project. Besides that, authors would like to thank for the financial support by UTeM Zamalah Scheme.

References

[1] T. Zou, B. Zhang and Y. Fan, "Design of a 73GHz waveguide bandpass filter," IEEE 9th UK-Europe-China Workshop on Millimetre Waves and Terahertz Technologies (UCMMT), Qingdao, 2016, pp. 219-221.

[2] A. Wahid and A. Munir, "Design of 9GHz dual-polarized rectangular waveguide antenna," 2nd International Conference on Wireless and Telematics (ICWT), Yogyakarta, 2016, pp. 44-46.

[3] K. Uyama, S. Nishimura, H. Deguchi and M. Tsuji, "Transmission characteristics of CRLH rectangular waveguides constructed by the cutoff modes of TM and TE waves," International Conference on Electromagnetics in Advanced Applications (ICEAA), Cairns, QLD, 2016, pp. 728-731.

[4] T. Rowe, P. Forbes, J. H. Booske and N. Behdad, "Inductive meandered metal line metamaterial for rectangular waveguide linings," *IEEE Transactions on Plasma Science*, vol. 45, no. 4, pp. 654-664, April 2017.

[5] B. Byrne, N. Raveu, N. Capet, G. Le Fur and L. Duchesne, "Field distribution of rectangular waveguides with anisotropic walls by using the modal theory," IEEE International Symposium on Antennas and Propagation (APSURSI), Fajardo, 2016, pp. 1091-1092.

[6] H. Sakli, D. Bouchouicha and T. Aguili, "Wave Propagation in Rectangular Waveguide Filled with Anisotropic Metamaterial," *IJCSI International Journal of Computer Science Issues*, vol. 9, issue 3, no. 3, May 2012.

[7] M. S. Alam, M. T. Islam and N. Misran, "Performance investigation of a uni-planar compact electromagnetic bandgap (UC-EBG) structure for wide bandgap characteristics," Asia-Pacific Symposium on Electromagnetic Compatibility, Singapore, 2012, pp. 637-640.

[8] M. S. Dalenjan, P. Rezaei, M. Akbari, S. Gupta and A. R. Sebak, "Radiation properties enhancement of a microstrip antenna using a new UC-EBG structure," 17th International Symposium on Antenna Technology and Applied Electromagnetics (ANTEM), Montreal, QC, 2016, pp. 1-2.

[9] D. Ferreira, R. F. d. S. Caldeirinha, I. Cuiñas and T. R. Fernandes, "Tunable square slot FSS EC modelling and optimisation," *IET Microwaves, Antennas & Propagation*, vol. 11, no. 5, pp. 737-742, 2017.

[10] G. S. Kunturkar and P. L. Zade, "Design of Fork-shaped Multiband Monopole antenna using defected ground structure," International

Conference on Communications and Signal Processing (ICCSP), Melmaruvathur, 2015, pp. 0281-0285.

[11] Z. Zakaria et al., "Compact structure of band-pass filter integrated with Defected Microstrip Structure (DMS) for wideband applications," The 8th European Conference on Antennas and Propagation (EuCAP 2014), The Hague, 2014, pp. 2158-2162.

[12] R. K. Shukla, Srinaga Nikhil N and K. J. Vinoy, "Radiation efficiencies of a compact planar antenna with different meander line configurations," IEEE Applied Electromagnetics Conference (AEMC), Guwahati, 2015, pp. 1-2.

[13] Y. Qi, J. Fan, Y. H. Bi, W. Yu and J. Drewniak, "A planar low-profile meander antenna design for wireless terminal achieving low self-interference," IEEE Symposium on Electromagnetic Compatibility and Signal Integrity, Santa Clara, CA, 2015, pp. 320-323.

[14] D. M. Pozar, *Microwave engineering*, 4th edition. New Jersey: John Wiley & Sons, INC, 2012.